JET AERATION STUDY BY FLOW VISUALIZATION METHOD WITH RHEOSCOPIC FLUID

Vladislav Yaroshevsky[1], Serhii Yasynskyi[1], Volodymyr Bulgakov[2],
Mariia Ruzhylo[2], Aivars Aboltins[3], Adolfs Rucins[3], Dmytro Polishchuk[4]
[1]Engineering and Technological Institute "Biotekhnika" of NAAS, Ukraine;
[2]National University of Life and Environmental Sciences of Ukraine, Ukraine;
[3]Latvia University of Life Sciences and Technologies, Latvia;
[4]Taras Shevchenko National University of Kyiv, Ukraine
wladscience@gmail.com, yasinskiy20@ukr.net , vbulgakov@meta.ua, masha.ruzhilo@ukr.net ,
aivars.aboltins@lbtu.lv, adolfs.rucins@lbtu.lv, dmytrosp@gmail.com

Abstract. The paper is devoted to investigating the jet aeration peculiarities in bioreactors based on the optical flow visualization method with rheoscopic fluid. The air distribution problem in fermentation medium in loop bioreactors aerated by jet devices is very actual for microbial cultivation but still insufficiently studied. The motion and mixing of air and fluid flows were studied in the jet aerator model of the jet loop bioreactor FT-0.325p for microbial pesticide manufacturing. The model represented the axial section of the jet aerator designed at a scale of 1:1 and made from an acrylic glass plate of 1.5 mm thickness. The jet aerator model was inserted between two thick acrylic glass plates (10 and 16 mm) containing flow channels for fluid and air supply and air-fluid mixture drain. The rheoscopic fluid was the water suspension of stearic acid (1:20 by mass). The fluid and pressured air were supplied to the model by a pump and air compressor respectively during the experiments. The fluid flow rate was changed from 2 to 6 $dm^3 \cdot min^{-1}$ with step of 1 $dm^3 \cdot min^{-1}$. The motion of the rheoscopic fluid and air-fluid mixing was caught on video on each value of fluid flow rate with simultaneous detection of flow static pressures and flow rates. Flow pattern analysis combined with estimated hydrodynamic parameters allowed us to evaluate the effect of initial flow conditions on mixing efficiency. At mixing of flows, air was distributed in the mixture as small air jets, packed into conglomerates, which were well seen on the frame-by-frame analysis of video records. The efficient aeration modes based on the well-aerated regions' size and location inside the aerator were identified with reference to the mixture flow regime. New data about air-fluid mixing can be the ground of the mathematical model development of jet aeration of fermentation medium in bioreactors.

Keywords: jet aeration, flow pattern, rheoscopic fluid, jet aerator model, flow visualization.

Introduction

The actual problem of different fermentation technologies is the aeration efficiency of fermentation medium in bioreactors. It is well known that oxygen volume dissolved in fermentation medium is one of the limiting parameters in submerged cultivation of aerobic bacteria and fungi. Therefore, different techniques of aeration and agitation are used for oxygen transfer intensification from air to fluid medium in bioreactors.

The jet aeration can be considered one of the most efficient aeration techniques [1; 2]. In fermentation technology, it is realized mostly in jet loop bioreactors [3; 4]. The main process of air saturation in the fluid medium for this bioreactor type takes place inside jet aerators. The ejectors are used as jet aerators in most cases, in which the fluid medium plays the role of the motive flow [1-4]. It is supplied to the aerator nozzle and the air is sucked due to the ejection effect. The medium and air are mixed in a jet aerator mixing chamber and then the mixture is transported to the bioreactor vessel [1; 3; 4].

In our previous work, we laid down another jet mixing scheme [5]. Both flows must be pressured according to it, and air sprayed into the fluid flow through the nozzle. Such an aeration technique allows for obtaining a well-aerated fermentation medium in the loop of a bioreactor, which has a much smaller diameter compared with a bioreactor vessel [5]. The tests of *Pseudomonas fluorescens* submerged cultivation in a 100 dm^3 jet loop bioreactor showed intensive growth of the bacteria culture compared to the bubble column of the same volume [6]. In our further work, we developed a 325 dm^3 bioreactor with the jet aerator of a similar design [7].

Despite the effectiveness of jet aeration, jet loop bioreactors are not widespread. One of the reasons for this, in our opinion, is insufficient information on the aeration process circumstances. The models of oxygen transfer in agitated bioreactors or bubble columns are based on the bubble size and lifting dynamic [8]. In jet aeration, the behaviour of separate bubbles could not be observed, so the model of

oxygen transfer could not be grounded on the same principle with another bioreactor type. The key to the model generation lays in the hydrodynamics understanding of air and fluid pressured flows mixing in a jet aerator. In this research, we have studied peculiarities of air and fluid mixing in jet aerators identified by the optical flow visualization method with rheoscopic fluid.

Materials and methods

The jet aerator of the jet loop bioreactor FT-0.325p for microbial pesticide manufacturing (ETI "Biotekhnika" NAAS) [6; 7] was chosen for modelling of air and fluid jet mixing by optical flow visualization. The jet aerator had the classical ejector form. It consisted of the nozzle, the chamber, and the Venturi tube with a cone, throat, and diffuser. The total length of the flow section was 214 mm. The diameters of air and fluid inlets as well as the mixture outlet were 20 mm. The nozzle diameter and Venturi tube diameters were 3 mm and 10 mm respectively. The model of the jet aerator was used in the research. The model represented the axial section of the jet aerator designed at a scale of 1:1 for geometrical similarity arrangement (Fig. 1).
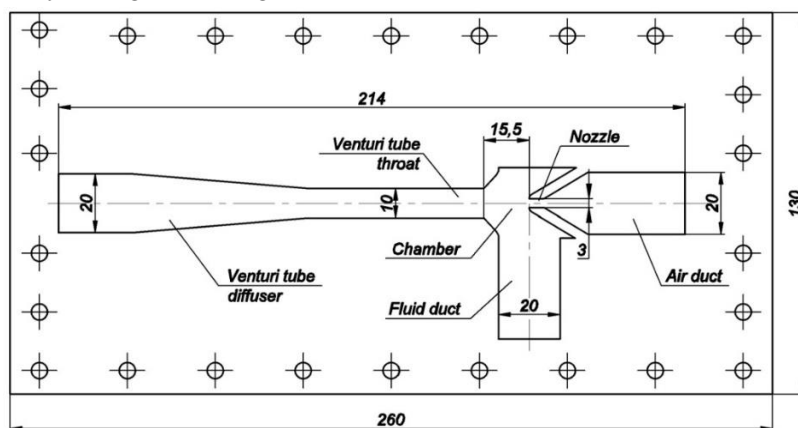

Fig. 1. **Model of jet aerator (dimensions in mm)**

It was made from an acrylic glass plate of 1.5 mm thickness defined according to J. Bychkov recommendations [9] on the base of a minimal stream tube width obtained by optical spot motion in preliminary tests made by flow visualization with rheoscopic fluid. The kinematic similarity of flows in the jet aerator and its model are provided with Reynolds number (Re_{mix}) of mixed flow, calculated by the average mass flow rate.

Flow visualization experiments were made at the experimental facility (Fig. 2).
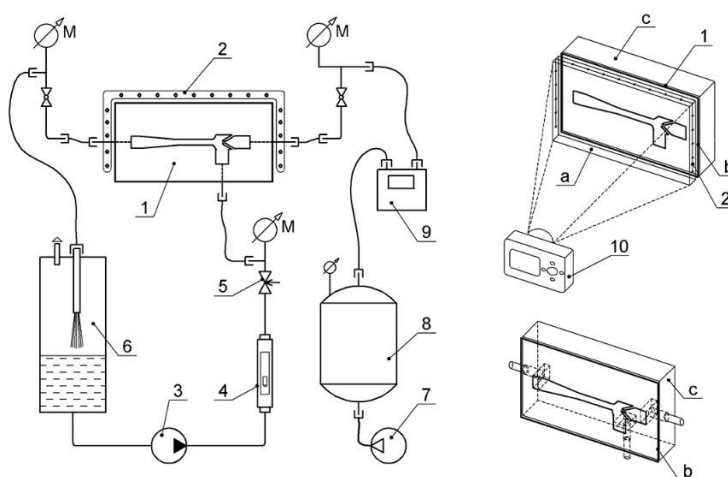

Fig. 2. **Experimental facility:** 1 – test section; 2 – LED strip; 3 – pump; 4 – fluid flowmeter; 5 – needle valve; 6 – fluid tank; 7 – air compressor; 8 – air receiver tank; 9 – air flowmeter; 10 – digital camera; M – pressure gauge. The structure of test section 1: a – front covering plate; b – model; c – back covering plate with flow channels

The main unit of the facility was the test section. It had a sandwich-type structure and consisted of two covering acrylic glass plates with the aerator model between them. The back plate contained flow channels for the rheoscopic fluid and air supply of the model and the air-fluid mixture drained from it. A non-transparent epoxide paper plate (getinaks) was encased between the back covering plate and the model, as fluid flow patterns could be visible only in refracted light.

The facility's fluid supply system consisted of a vortex pump (Koer KP.P15-GRS 10), a flowmeter (Kobold DSV-1104H.00.R15), a needle valve, and a 10 dm^3 glass tank for rheoscopic fluid accumulation. The air supply system contained a reciprocating compressor (Resun ACO-012), a 10 dm^3 air receiver tank for pressure pulsation damping, and a flowmeter (Metrix).

A LED strip placed around the test section covering plate illuminated the motion of the fluid and air-fluid mixture. A digital camera (Canon PowerShot SX412 IS) detected flow patterns in the model.

The rheoscopic fluid was a water suspension of stearic acid (1:20 by mass) prepared by the D. Borrero-Echeverry technique [10]. The fluid density at 24 °C was 0.972 g·cm^{-3}, and the kinematic viscosity coefficient was 0.926·10^{-6} m^2·s^{-1}. Thus, the difference in properties of the rheoscopic fluid and water did not exceed 4% at the same temperature.

Rheoscopic fluid and pressured air were supplied to the test section by a pump and air compressor respectively during the experiments. The fluid flow rate (Q_f) was changed from 2 to 6 dm^3·min^{-1} with a step of 1 dm^3·min^{-1} by a flow orifice with a needle valve. The mixing process of flows in the model was caught on video on each value of the fluid flow rate. Flow meters and pressure gauge indications were detected by two additional digital cameras at the same time for obtaining transient values of flow rates and pressures which should stand for flow patterns in the model. The experiment was made in triple. The data from video recordings were obtained by Vegas Pro. 20.0 software.

Flow pattern dynamics analysis was made at images obtained from video records (frame-by-frame method) at different Reynolds numbers. The thickness of flow pattern different layers was determined by their dimensioning in AutoCAD 2024 software environment.

Jet aeration mode was determined on the basis of our previous work [5] by the dependence between dimensionless flow rate and dimensionless total pressure. The dimensionless flow rate q calculated as a ratio of volumetric flow rates of fluid and air, and the dimensionless total pressure p was the ratio of total pressures of air and fluid. Statistical analysis of flow parameters was made in MS Excel by standard technique [11]. Arithmetic means of pressures and flow rates, and standard deviations were found. Relative and absolute measurement errors were calculated for 95% confidence.

Results and discussion

General view of flow patterns

The optical flow visualization experiments resulted in flow patterns of the air and rheoscopic fluid in the jet aerator model, a general view of which is represented in Fig. 3.
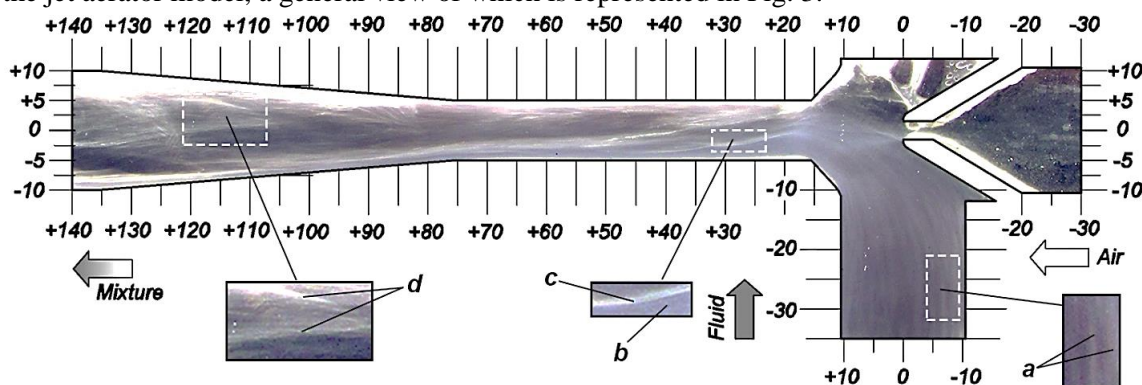

Fig. 3. **General view of flow patterns in air and rheoscopic fluid mixing at Remix = 5000 (the scale in mm):** a – optical spots in rheoscopic fluid flow; b – unmixed fluid; c – boundary between fluid and air-fluid mixture; d – air small jets

The number of flow peculiarities could be identified and studied by flow pattern analysis: localization and shape of the air and fluid flow before mixing started; regions with intensive and passive

air-fluid mixing; separate air small jets in the air-fluid mixture; boundaries between the fluid and air-fluid mixture; optical spots in the rheoscopic fluid flow indicated stream tube motion [9] etc.

As one can see, flow visualization with the rheoscopic fluid on the basis of the stearic acid suspension allows to obtain sharply defined flow patterns, which meet or exceed ones gained not only by stearic acid-based suspensions [10] but by rheoscopic fluids of another content [12], as well as colloidal solution of vanadium pentoxide [9, 13] and suspensions of bentonites [14]. On the other hand, usage of the stearic acid rheoscopic fluid has no special requirements for pipes, valves, tanks, and materials. It is tolerant to aggregation of particles as opposed to the vanadium pentoxide colloidal solution [9, 13]. This significantly simplifies experimental facilities design and experimentation. Moreover, the preparation of stearic acid-based rheoscopic fluids [10] is much easier and cheaper than other colloidal solutions [9] or suspensions [12, 14].

Fluid and air flow interaction before mixing

The jet mixing process predetermines the flow regimes of air and fluid upstream of the jet aerator. The effect of flow interaction in the aerator model on the parameters of air and fluid streams was studied in the fluid flow rate changes. It was found that the fluid flow rate increasing came with its static pressure increasing, and led to the air flow rate reduction with the air static pressure increasing. Rheoscopic fluid flow rate (Q_f) increased from 2 to 6 dm^3·min^{-1} initiated the air flow rate (Q_a) reduction from 12.5 to 1.2 dm^3·min^{-1}, with the same the static pressure increased from 16 to 35 kPa for fluid ($P_{st\,f}$) and from 19 to 25 kPa for airflow ($P_{st\,a}$).

Thus, the fluid flow was throttling the air flow in the jet aerator chamber. Air velocity decreasing attended with pressure increasing was observed, i. e. the air flow kinetic energy reduction went with potential energy increasing. This transformation of air stream energy must be reflected in the flow pattern. Therefore, the analysis of flow patterns in the chamber of the aerator model at different combinations of flow parameters was made (Fig. 4).
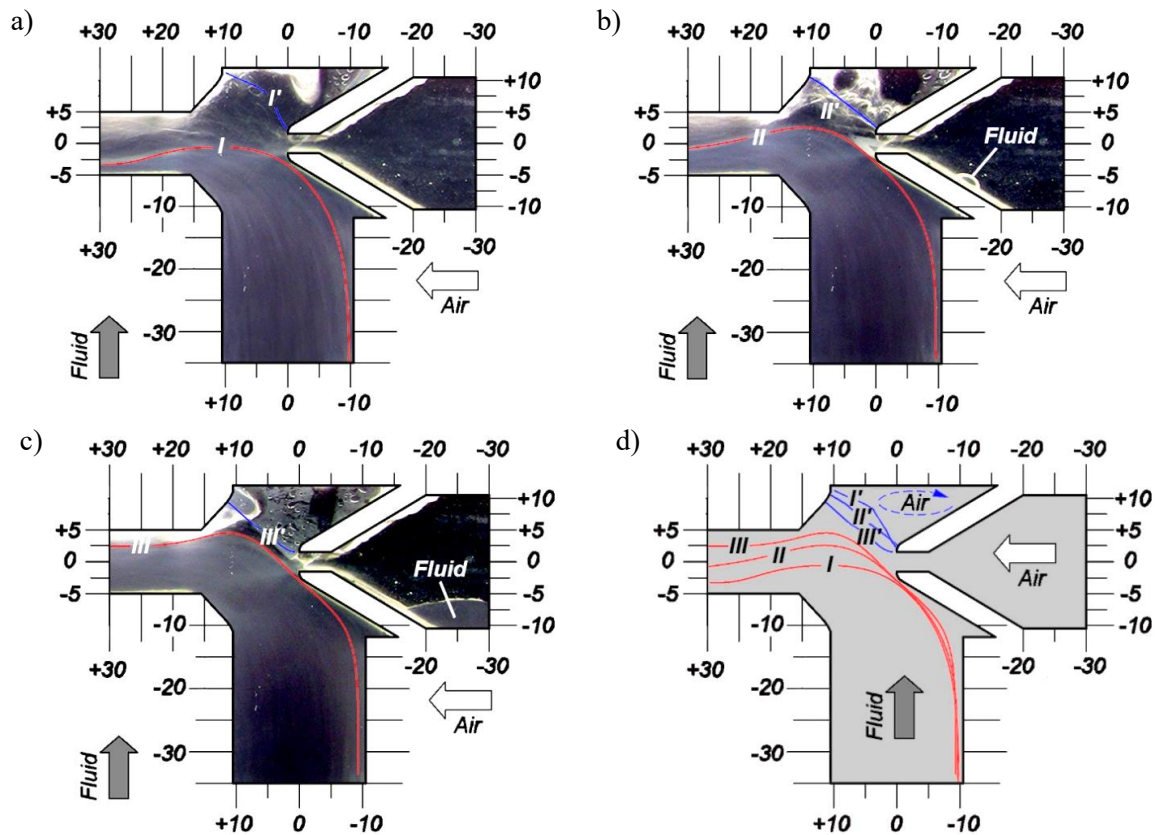
Fig. 4. **Flow patterns in jet aerator chamber model at different flow regimes (the scale in mm):**
a – $P_{st\,a}$ = 20 kPa, Q_a = 9.6 dm^3·min^{-1}, $P_{st\,f}$ = 19 kPa, Q_f = 2.2 dm^3·min^{-1}; b – $P_{st\,a}$ = 24 kPa,
Q_a = 3.1 dm^3·min^{-1}, $P_{st\,f}$ = 27 kPa, Q_f = 4.2 dm^3·min^{-1}; c – $P_{st\,a}$ = 26 kPa, Q_a = 1.2 dm^3·min^{-1},
$P_{st\,f}$ = 35 kPa, Q_f = 6.5 dm^3·min^{-1}; d – the edges of rheoscopic fluid flow (red lines I-III)
and air circulation zone (blue lines I'-III')

As one can see the edge of the rheoscopic fluid flow (red lines I-III) was approached to the Venturi tube throat with the flow rate and pressure of the fluid increasing. That caused to clear opening for the air flow, supplied to the chamber through the nozzle, decreasing from 2/5 to 1/10 of the Venturi tube throat cross-section (10 mm). Therefore, the air flow rate connected with its dynamic pressure (kinetic energy of the flow) was reduced. At the same time a part of the air, which could not pass through the Venturi tube, stayed at the chamber and circulated at the zone located above the nozzle, additionally resisting the air flow inlet. The size of the circulation zone increased with the air flow rate reduced (blue lines I'-III'). Such changes in the air flow patterns led to the air static pressure (potential energy of the flow) increasing. Hence, the optical visualization technique allowed for graphical representation of changes in the flow parameters of air and fluid in different flow regimes.

It should be noted that the fluid could get into the air duct through the nozzle at some flow regimes (Fig. 4 b, c). The pressure difference between the fluid and air flows required for this was 2.5-2.8 kPa reached with the fluid flow rate $Q_{f>}$ 3.8 dm^3·min^{-1}. The fermentation medium getting into the air duct is very unwanted in the jet aerator operation at a bioreactor loop and must be avoided. Therefore, a non-return valve should be set upstream of the aerator nozzle inlet.

Jet mixing of air and fluid flows

The peculiarities of air and fluid jet mixing were studied by flow patterns analysis in the Venturi tube (Fig. 5). The mixing process took place in turbulent flow mixture regimes in the model, and the Reynolds number (Re$_{mix}$) varied from 3300 to 10000. The air was mixed into the rheoscopic fluid flow with air-fluid conglomerate generation. The conglomerate contained small air jets and larger fluid jets. The conglomerates were generated in the Venturi tube by contact of the air and fluid flows.
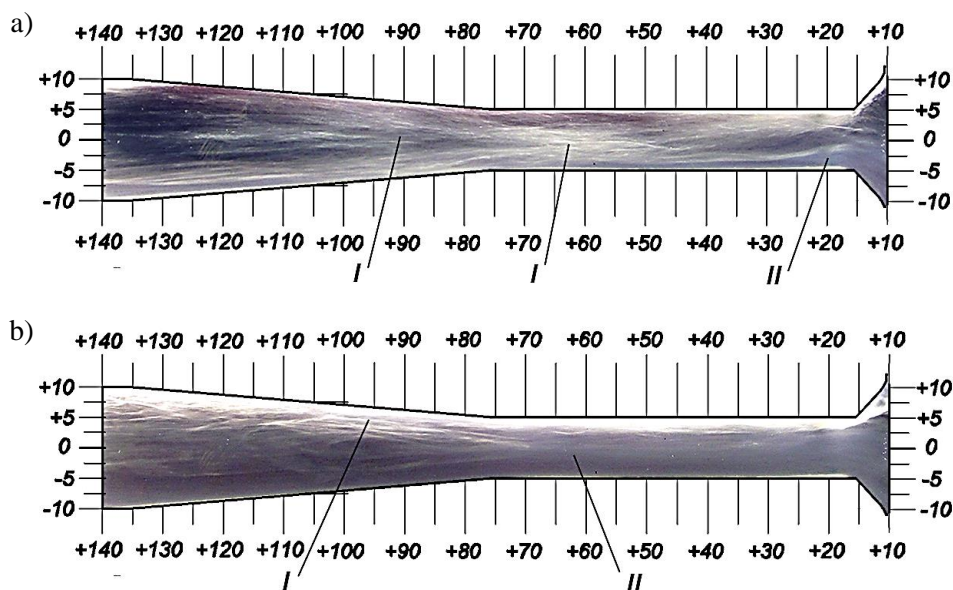

Fig. 5. **Flow patterns in jet aerator Venturi tube model at different flow regimes (the scale in mm):** a – $P_{st\,a}$ = 20 kPa, Q_a = 9.6 dm^3·min^{-1}, $P_{st\,f}$ = 19 kPa, Q_f = 2.2 dm^3·min^{-1}, Re$_{mix}$ = 3300; b – $P_{st\,a}$ = 26 kPa, Q_a = 1.2 dm^3·min^{-1}, $P_{st\,f}$ = 35 kPa, Q_f = 6.5 dm^3·min^{-1}, Re$_{mix}$ = 10000; I – air-fluid conglomerate (well-mixed region); II – rheoscopic fluid flow (unmixed region)

The frame-by-frame analysis of video records showed the dynamic of air-fluid conglomerate creation and motion. The separate conglomerate was generated when the air flow blew a batch of fluid at the phase's contact. This fluid batch was instantaneously saturated by air. The created conglomerate consisted of small air jets (0.3 mm thick) and fluid among them. It could move downstream as a separate structure or join other conglomerates in a predetermined air-fluid mixture flow pattern.

Another component of flow patterns in the Venturi tube was the regions of unmixed fluid flow. They occupied the lower part of the Venturi tube in all regimes. The region thickness increased with th fluid flow rate (and corresponding Re$_{mix}$). However, the unmixed fluid flow thickness increased sharply at Re$_{mix}$ = 8500. Above this value, it occupied almost half of the Venturi tube space.

Thus, the Venturi tube contained well-mixed regions with air-fluid conglomerates, and unmixed regions with the rheoscopic fluid flow. It can be said that the efficiency of jet aeration depended on the ratio of well-mixed to unmixed region volume at the Venturi tube. Flow pattern analysis showed that changes in this ratio varied with the fluid flow rate and corresponding mixture motion regime evaluated by Re_{mix}.

At $Re_{mix} < 8500$ ($Q_{f < }5$ dm^3·min^{-1}) 76-82% of Venturi tube space was occupied by air-fluid conglomerates and unmixed fluid flow low thickness (1.5-3 mm). The jet aeration process started in the throat inlet and developed through the Venturi tube length. Therefore, it could be considered as effective.

At $Re_{mix} > 8500$ ($Q_{f >} 5$ dm^3·min^{-1}) the jet aeration efficiency reduced significantly. Mixing started in the throat outlet developed only in the Venturi tube diffuser. Unmixed fluid flow occupied almost 50% of the Venturi tube space. Such matter could be explained by the conditions of the air and fluid flows supplied into the Venturi tube inlet, described above. Clear opening for the air flow in the Venturi tube throat was considerably reduced with the fluid flow rate and pressure increasing up to 5 dm^3·min^{-1} and 30 kPa respectively ($Re_{mix} = 8500$). That caused the air flow rate reduction and a corresponding decrease of the air-fluid contact surface in the Venturi tube.

These results could be depicted in the jet aeration mode diagram [5] by dimensionless flow parameters (Fig. 6). The mode of aeration in the model was plotted by averaging three test series.
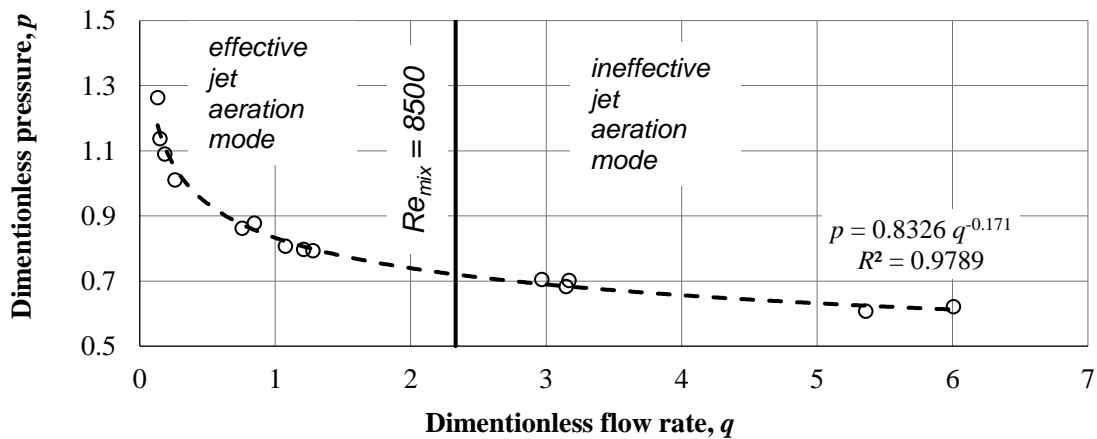

Fig. 6. **Jet aeration mode**

A general configuration of the dependence between the dimensionless flow rate q and pressure p correlates with ones obtained in our previous work [5]. However, the diagram contains information about effective modes of the jet aerator which could not be obtained without flow visualization.

Conclusions

1. Hydrodynamic peculiarities of air and fluid pressured flows mixing in the jet aerator obtained by optical flow visualization allow identification of effective and ineffective modes of aeration. Such information cannot be received on the base of quotative evaluation of flow parameters only. Effective jet aeration modes can be used for aeration and agitation setting development of jet loop bioreactors.
2. There was first described air-fluid conglomerate generation at jet aeration. The obtained data can be the ground for a mathematical model development of jet aeration.
3. Optical flow visualization with rheoscopic fluid can be a powerful tool for understanding and describing hydrodynamic processes at different devices and equipment.
4. Our further research will be focused on experimental verification of jet aeration modes obtained for the aerator model on a real jet aerator of a bioreactor.

Author contributions

Conceptualization, V.B.; A.A.; methodology, V.B. and A.A.; A.R.; software, S.Y.; D.P.; validation, A.A.; A.R.; and V.B; formal analysis, A.A.; A.R.; and V.Y.; investigation, V.Y. and S.Y.; data curation, V.Y. and V.B.; writing–original draft preparation, V.Y.; writing–review and editing, A.A.; V.B.; and

References

[1] Weber S., Schaepe S., Kopf M.-H, Freyer S., Dietzsch C. Jet aeration as alternative to overcome mass transfer limitation of stirred bioreactors. Chemie Ingenieur Technik, 2018, vol. 90, pp. 1250-1250. DOI: 10.1002/cite.201855260.

[2] Radkevich M., Abdukodirova M., Shipilova K., Abdullaev B. Determination of the optimal parameters of the jet aeration. 2nd International conference on energetics, civil and agricultural engineering 2021 (ICECAE 2021) October, 14-16, 2021, Tashkent, Uzbekistan. IOP Conference Series "Earth and Environmental Science", vol. 939, 2021. 012029. DOI: 10.1088/1755-1315/939/1/012029.

[3] Ughetti M., Jussen D., Riedlberger P. The ejector loop reactor: Application for microbial fermentation and comparison with a stirred-tank bioreactor. Engineering in Life Science, vol. 18(5), 2018, pp. 281-286. DOI: 10.1002/elsc.201700141.

[4] Meyer H., Charles M. Cultivation of a filamentous bacterium in a deep jet fermentor. Biotechnology and Bioengineering, vol. 24, 1982, pp. 1905-1909. DOI: 10.1002/bit.260240819

[5] Yaroshevsky V., Krutyakova V., Belchenko V., Ivanovs S., Bulgakov V. Development and research of new media jet aeration scheme in a loop bioreactor producing microbiological products. Acta Technologica Agriculturae. vol. 24, 2021, pp. 124-128. DOI: 10.2478/ata-2021-0021.

[6] Беспалов І.М., Ярошевський В.П. Економічна ферментаційна установка для виробництва мікробіологічних засобів захисту рослин. Системи виробництва і застосування засобів біологізації землеробства: монографія. (The economic fermentation unit for microbial plant protection products. In the systems of agriculture biologization agents manufacturing and using: monograph), Київ: Аграрна наука, 2022, pp. 100-121. DOI: 10.31073/ 978-966-540-558-0 (In Ukrainian)

[7] Ходорчук В.Я., Ярошевський В.П. Технологічний проєкт ферментаційної установки для малотоннажного виробництва мікробіологічних засобів захисту рослин (The engineering design of fermentation unit for microbial plant protection products small-scale manufacturing) Механізація і електрифікація сільського господарства, vol. 13(112), 2021. pp. 65-72. DOI: 10.37204/0131-2189-2021-13-6 (In Ukrainian)

[8] Luo H., Svendsen H.F. Theoretical model for drop and bubble breakup in turbulent dispersions. AICHE Journal, vol. 42(5), 1996, pp.1225-1233 DOI: 10.1002/aic.690420505.

[9] Бычков Ю.М. Визуализация тонких потоков несжимаемой жидкости (The visualization of thin incompressible fluid flows), Кишинев: Штиинца, 1980. 132 p. (In Russian)

[10] Borrero-Echeverry D., Crowley C.J., Riddick T.P. Rheoscopic fluids in a post-Kalliroscope world Physics of Fluids. vol. 30, 2018, 087103. DOI: 10.1063/1.5045053

[11] Divisi D., Di Leonardo G., Zaccagna G., Crisci R. Basic statistics with Microsoft Excel. Journal of Thoracic Disease, vol. 9(6), 2017, pp. 1734-1740. DOI: 10.21037/jtd.2017.05.81.

[12] Abcha N., Latrache N., Dumouchel F., Mutabazi I. Qualitative relation between reflected light intensity by Kalliroscope flakes and velocity field in the Couette-Taylor flow system. Experiments in Fluids, vol. 45, 2008, pp. 85-94. DOI: 10.1007/s00348-008-0465-9.

[13] Арсирий В.А., Ковальчук Ю.Г., Григорук И.В. Улучшение работы гидравлического оборудования на основе совершенствования структуры потоков (Hydraulic equipment operation improvement on the basis of flow patterns optimization). Гідроенергетика України, vol. 3-4, 2018. pp. 42-45. Available at: http://nbuv.gov.ua/UJRN/gidenu_2018_3-4_13 (In Russian)

[14] Meisner J.E., Rushmer R.F. Eddy Formation and Turbulence in Flowing Liquids. Circulation Research, vol. 12, 1963, pp. 455-463. DOI: 10.1161/01.RES.12.5.455